JOURNAL OF SPACECRAFT AND ROCKETS
Vol. 40, No. 3, May–June 2003

Simulation of Dual One-Way Ranging Measurements

Jeongrae Kim* and Byron D. Tapley†
University of Texas at Austin, Austin, Texas 78759

One of the main error sources for the microwave ranging method is the frequency instability of the oscillator that generates the carrier phase signal. A dual one-way ranging method is used to minimize the oscillator noise effect by combining two one-way ranging measurements. This study analyzed the dual one-way ranging system by simulation of the phase measurements with comprehensive error models. This simulation analysis was applied to the Gravity Recovery and Climate Experiment mission, which is a dedicated spaceborne mission with the objective of mapping the gravity field. The simulation results demonstrate that a high level of accuracy can be achieved by use of the dual one-way ranging system.

Nomenclature

c	=	speed of light, m/s
d	=	satellite center of mass to antenna phase center offset, m
f	=	frequency, Hz
$\bar{f}$	=	reference frequency, Hz
I	=	lonosphere effect, cycle
N	=	phase ambiguity, cycle
R	=	dual one-way range, m
t	=	nominal observation time, s
Δt	=	time-tag error, s
δf	=	frequency error, Hz
$\delta\varphi$	=	phase error, cycle
ε	=	phase measurement noise, cycle
Θ	=	dual one-way phase, cycle
λ	=	signal wavelength, m
ρ	=	instantaneous intersatellite range, m
τ	=	signal time of flight, s
φ	=	phase measurement, cycle
$\bar{\varphi}$	=	reference phase, cycle

Introduction

THERE has been increasing interest in satellite formation flying in recent years, with the corresponding need for measuring the intersatellite distance with high accuracy. One of the ways of measuring the intersatellite distance is the use of an intersatellite microwave ranging system to count the number of carrier phases. The accuracy of this type of system is mainly limited by the instability of the oscillator that drives the phase signals.

A dual one-way ranging system minimizes the oscillator noise effect by combining the one-way range measurements from two microwave ranging systems. With identical transmission and reception subsystems, each satellite transmits a carrier phase signal to the other satellite. The received signal at each of the two satellites is recorded and later transmitted to a control segment, for example, a ground station. The frequency fluctuations due to oscillator instability have nearly equal and opposite effects on each satellite's measurement, and summation of these two phases cancels most of the oscillator noise. The combined phase measurement is converted to the biased range between the two satellites with very high precision.

In the 1980s, this type of the dual one-way ranging system was first studied by the Johns Hopkins University, Applied Physics Laboratory for the NASA Geopotential Research Mission (GRM), which was to be a dedicated spaceborne mission designed to map the gravity field with high accuracy.[1–3] The orbit of any satellite in a near Earth orbit depends on the globally integrated effect of mass distributions, as well as mass movement in the Earth's systems. The orbits of two coorbiting satellites, sensing these effects at slightly different phases, will be perturbed differentially. This difference in perturbations is manifested in the intersatellite range change, and the need for measuring this range change with very high accuracy was a motivation for developing the dual one-way ranging system.[4–6] However, the GRM mission was canceled, and this ranging system did not have the chance to fly.

In 1997, the Gravity Recovery and Climate Experiment (GRACE) was selected under the NASA Earth System Science Pathfinder program.[7] Similar to the proposed GRM mission, the GRACE mission utilizes high-accuracy intersatellite ranging measurements between two coorbiting satellites. The two satellites are separated in orbit by 220 ± 50 km along track. The orbit inclination is close to 90 deg, and the initial altitude is 500 km. This relatively low orbit altitude makes it possible to detect high-frequency temporal and spatial gravity signals. To correct the signal delay due to the ionosphere, two frequency signals, K (24 GHz) and K_a (32 GHz) bands, are used.

The satellite orbit is affected not only by the gravitational accelerations, but also by nongravitational accelerations, for example, atmospheric drag and radiation pressure, and their effects must be accurately measured and corrected to extract the gravitational information in the range change measurements. For this purpose, the GRACE satellites carry high-precision three-axis accelerometers. Each satellite also carries a geodetic quality global positioning system (GPS) receiver to ensure that the positions of the satellites can be continuously and accurately determined, so that the gravity field estimates can be correctly registered in a terrestrial reference frame.

The GRACE mission is implemented under the overall direction of the University of Texas Center for Space Research. The NASA Jet Propulsion Laboratory (JPL), California Institute of Technology, has been assigned responsibility for the development of the science instrument and satellite system in partnership with Space Systems/Loral and Dornier Satellitensysteme. Two GRACE satellites were sucessfully launched in March 2002 and started their five-year mission.

To support the dual one-way system hardware developments, a series of analytic and numerical analyses have been performed; ranging performance prediction, filtering characteristics, etc. Most of the previous analytic analyses used a spectral domain approach.[1,8] and the instrument error analyses were limited to certain types of error

Received 6 July 2002; revision received 28 February 2003; accepted for publication 2 March 2003.

*Research Associate, Center for Space Research; currently Senior Researcher, Guidance and Control Department, Korea Aerospace Research Institute, Daejon 305-333, Republic of Korea; jeongrae@kari.re.kr. Senior Member AIAA.

†Clare Cockrell Williams Chair and Director, Center for Space Research; tapley@csr.utexas.edu. Fellow AIAA.

sources and assumptions. To overcome these limitations, a software simulator has been developed. This paper describes the algorithm and results of the software simulator. The simulator generates the phase measurement time series and then processes them to extract the intersatellite ranging information. All of the processes were done in the time domain, and use of this time domain approach made it possible to apply more extensive error models than the analytic or spectral approach. Furthermore, the time-domain results allowed us to validate the analytic and spectral analysis results. This simulation study was specifically applied for the GRACE mission, but it can be applied to other dual one-way intersatellite ranging systems by a change of appropriate simulation parameters, for example, carrier frequencies and separation distance.

Measurement Equations

Intersatellite Ranging Observable

The dual one-way ranging system measures the low–low intersatellite range, plus some noise and corrections. The intersatellite range equation can be expressed as[9]

$$\rho(t) = \sqrt{[\boldsymbol{r}_1(t) - \boldsymbol{r}_2(t)] \cdot [\boldsymbol{r}_1(t) - \boldsymbol{r}_2(t)]} \tag{1}$$

where the position vectors of satellite 1 and 2 are defined as $\boldsymbol{r}_1$ and $\boldsymbol{r}_2$, respectively. This range represents an instantaneous range at the nominal time t. This quantity is different from the range measurement inferred from the phase measurements by multiplication of the wavelength, which contains a finite time of flight for the signal, time-tag errors, instrument bias, etc. Use of this instantaneous quantity allows a more direct implementation of the estimation algorithm. The dual one-way ranging model in the next section converts the observed phases into this instantaneous range in a manner that accounts for the major effects associated with true terms of flight measurements.

Dual One-Way Ranging

The following formulations describe how to obtain the instantaneous range of Eq. (1) from the one-way phase measurements. This derivation shows how the oscillator noise from the individual spacecraft is canceled out through the use of the dual one-way ranging.

Figure 1 illustrates the phase measurements from the dual one-way ranging system. The output from each satellite is the one-way phase measurement, and this is sent to the ground for processing. The single-frequency carrier phase measurement received at the ith satellite at a specified nominal time t can be modeled as follows[8,10,11]:

$$\varphi_i^j(t + \Delta t_i) = \varphi_i(t + \Delta t_i) - \varphi^j(t + \Delta t_i) + N_i^j + I_i^j + d_i^j + \varepsilon_i^j$$
$$i, j = 1, 2, \qquad i \neq j \tag{2}$$

This is the difference between the reference phase of the ith satellite, $\varphi_i\ (t + \Delta t_i)$, and the received phase from the jth satellite, $\varphi^j\ (t + \Delta t_i)$, with the time-tag error of Δt_i. This measurement contains the integer ambiguity N_i^j, ionosphere phase shift I_i^j, phase shift due to other effects d_i^j, and measurement noise ε_i^j. This carrier phase travels from the antenna phase center (PC) of one satellite to the PC of the other satellite. This phase equation corresponds to the PC-to-PC range, but it can be converted into a satellite center of mass c.m.-to-c.m. range with the known offset d_i^j.

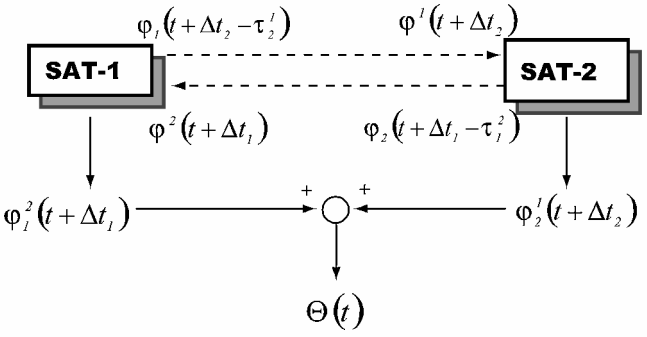

Fig. 1 Phase measurements of the dual one-way ranging system.

A dual one-way phase measurement for K or K_a band is defined as the sum of two one-way phases:

$$\Theta(t) \equiv \varphi_1^2(t + \Delta t_1) + \varphi_2^1(t + \Delta t_2) \tag{3}$$

for the K or K_a band. For measurement error analysis, this equation can be expanded after appropriate substitutions and approximations are made. The received phase φ^j can be replaced with the transmitted phase φ_j at the transmit time:

$$\varphi^j(t + \Delta t_i) = \varphi_j\left(t + \Delta t_i - \tau_i^j\right) \tag{4}$$

where τ_i^j is the time of flight from the jth satellite to the ith satellite. Each phase $\varphi_i(t)$ can be decomposed into the reference phase $\bar{\varphi}_i$ and the phase error $\delta\varphi_i$ due to the oscillator instability. The rate of phase change $\dot{\bar{\varphi}}_i\ (t)$ can be replaced with the constant nominal frequency $\bar{f}_i$. The carrier frequencies from the two satellites are slightly different by design and denoted by f_1 and f_2. After these substitutions, the dual one-way phase can be approximated by

$$\Theta(t) = \left(\bar{f}_1\tau_2^1 + \bar{f}_2\tau_1^2\right) + \left\{\left[\delta\varphi_1(t) - \delta\varphi_1\left(t - \tau_2^1\right)\right]\right.$$
$$\left. + \left[\delta\varphi_2(t) - \delta\varphi_2\left(t - \tau_1^2\right)\right]\right\} + (\bar{f}_1 - \bar{f}_2)(\Delta t_1 - \Delta t_2)$$
$$+ (\delta\dot{\varphi}_1 - \delta\dot{\varphi}_2)(\Delta t_1 - \Delta t_2) + N + I + d + \varepsilon \tag{5}$$

The first term represents the true phase measurement, the second term represents the phase error due to the oscillator errors, the third term is due to the time tag errors, and the fourth term is the coupling between the oscillator and time-tag errors. The remaining terms represent the combined effects of the two satellites for previously defined quantities, for example, $N = N_1^2 + N_2^1$. Note that the second term represents the phase error difference over the time of flight τ_1^2 or τ_2^1. This implies that the long and medium period phase error, which has a period longer than the time of flight ($\sim$1 ms), can be removed by this dual one-way combination. This noise reduction method is similar to the GPS differencing technique.[10]

The two times of flight, τ_2^1 and τ_1^2, in Eq. (5) can be converted into a single time of flight (TOF) corresponding to the instantaneous range $\rho\ (t)$ by the use of

$$\left(\bar{f}_1\tau_2^1 + \bar{f}_2\tau_1^2\right) \approx (\bar{f}_1 + \bar{f}_2)\tau + \Delta\Theta_{\mathrm{TOF}}(t), \qquad \tau = \rho(t)/c \tag{6}$$

where $\Delta\Theta_{\mathrm{TOF}}$ is called a light-time range correction. This light-time range correction is similar to the conventional light-time correction[10] and can be computed from the nominal (or preliminary) orbits with sufficient accuracy.[11]

The dual one-way phase is converted to a dual one-way range by multiplication with an effective wavelength λ:

$$R(t) \equiv \lambda\Theta(t), \qquad \text{where} \qquad \lambda = c/(\bar{f}_1 + \bar{f}_2) \tag{7}$$

Substitution of Eqs. (5) and (6) into Eq. (7) yields the instantaneous range equation for K or K_a band at the time t that relates the instantaneous range $\rho(t)$ to the dual one-way range measurement $R(t)$:

$$R(t) = \rho(t) + \rho_{\mathrm{TOF}}(t) + \rho_{\mathrm{err}}(t) + N' + I' + d' + \varepsilon' \tag{8}$$

for the K or K_a band, where ρ_{TOF} is the light-time range correction and ρ_{err} is the range error due to the oscillator and time-tag errors. The remaining terms N', I', d', and ε' are obtained by scaling N, I, d, and ε with λ. Because this equation is for either the K or K_a band, there are two dual one-way ranges, R_K and R_{K_a}.

The last step is to eliminate the ionosphere effect I by the use of the conventional ionosphere-free combination[8]:

$$R = \frac{\bar{f}_K^2 R_K - \bar{f}_{K_a}^2 R_{K_a}}{\bar{f}_K^2 - \bar{f}_{K_a}^2} \tag{9}$$

Because there is an offset between the two satellites' transmit frequencies, the effective frequency $\bar{f}$, which is the geometric mean of two satellites' frequencies for each band, is used. In summary, the one-way phases $\varphi_i^j(t + \Delta t_i)$ of Eq. (2) are converted into the instantaneous range $\rho(t)$ of Eq. (8), except for the noise and ambiguity components.

Measurement Error Sources

This section describes the individual error sources in the one-way phase measurement of Eq. (2). The effects of the oscillator noise and time-tag error on the dual one-way phase are also analyzed with Eq. (5). The realization of these errors will be described in the Simulation Description section.

The oscillator noise or instability $\delta\varphi_i$ affects the phase φ_i directly but can be reduced after the dual one-way ranging filtering. The oscillator noise residual after the filtering is called the oscillator noise in this study, and it is identified as the second term in Eq. (5). Its error level depends on the oscillator characteristics and the efficiency of the dual one-way ranging filtering. (The latter is mainly a function of satellite separation distance.) A shorter separation distance is better for the noise cancellation because it reduces the signal TOF.

The time-tag error in this study represents the time-tag error residual after the time-tag correction process on the ground, not the initial time-tag error onboard. With the GPS data, the measurement time-tag can be determined very accurately after the ground processing. Then, each one-way measurement is interpolated toward the nominal time t, and the original time-tag error Δt_i can be replaced with a much smaller value. Specifically, the relative time-tag error, $(\Delta t_1 - \Delta t_2)$, becomes much smaller because most of common time-tag errors are canceled. The dual one-way phase error due to the time-tag error [third term of Eq. (5)] is related to the relative time-tag error between the two satellites, not the absolute errors. A smaller frequency offset $(f_1 - f_2)$ reduces the range/phase error as shown in the equation. Because the observable is an inherently biased range due to the phase ambiguities, the variability of the time-tag error is of primary interest, rather than its absolute value.

The measurement noise ε_i^j [last term of Eq. (2)] may include system noise, multipath error, and phase modulation error:

$$\varepsilon_{\text{true}} = \varepsilon_{\text{system}} + \varepsilon_{\text{multipath}} + \varepsilon_{\text{AM/PM}} + \text{other} \tag{10}$$

The system noise $\varepsilon_{\text{system}}$ is due to the receiver instrument noise, and its mean value is mainly dependent on the distance between the two satellites or the signal-to-noise ratio (SNR). The multipath error $\varepsilon_{\text{multipath}}$ is due to the indirect received signals when the line of sight (LOS) of the two satellites is not perfectly aligned with the microwave antenna boresight. This error may be a function of the satellite geometry and attitude control characteristics. During the extraction of the phase signal from the incoming microwave signal, amplitude modulation/phase modulation (AM/PM) error $\varepsilon_{\text{AM/PM}}$ is generated due to the variation of the incoming signal strength. This variation is mainly dependent on the SNR or the intersatellite distance, and it can be modeled as proportional to the range variation. All of these measurement errors are applied to the truth phase measurements, but no corresponding error models are applied for the range estimation process.

The offset term d_i^j of Eq. (2) represents the sum of the phase shifts, which is related to the distance between the c.m. of the satellites and the PC of the satellite microwave antenna. The phase measurements reflect the distance between the PC of the two satellites. For orbit and gravity estimations, this distance needs to be converted into the distance between the c.m. of the satellites. The offset d is used to convert the PC-to-PC range into the c.m.-to-c.m. range. The offset error can be realized by differencing the simulated and estimated offsets $(d_{\text{true}} - d_{\text{nominal}})$

$$d_{\text{true}} = d_{\text{true attitude}} + d_{\text{thermal}}$$

$$d_{\text{nominal}} = d_{\text{nominal attitude}} + (d_{\text{nominal thermal}}) \tag{11}$$

where the indices of d_i^j are dropped for simplicity. The conversion from the PC-to-PC range into the c.m.-to-c.m. range involves the projection of each satellite's c.m.-to-PC vectors along the c.m.-to-c.m. vector, or LOS vector. Because of the long baseline between the two GRACE satellites (~220 km), the LOS vector direction can be well determined in spite of the modest nominal orbit error (<50 cm). Therefore, the conversion accuracy is dominated by the c.m.-to-PC vector accuracy. The directions of these vectors are derived from the attitude measurements by the star cameras. Unlike the multipath error, which depends only on the attitude control accuracy, this error depends on the attitude knowledge accuracy as well.

Another critical error source is the c.m.-to-PC distance variation due to thermal distortion, which includes mechanical distortion and PC variation, and this type of error degrades the range accuracy directly. The simulator has a capability to apply the thermal distortion error to the phase measurements using either a user-specified thermal distortion time series or with an internal analytically generated time series. However, this error level mostly depends on the structure design and thermal control methodology specific to a satellite. Because this study focused on the dual one-way ranging system itself, the results in this paper do not include the thermal distortion effect.

Simulation Procedure

The simulation procedure consists of two parts, measurement simulation and measurement processing. The output from the first part is a set of four one-way phase measurements for each epoch. The second part extracts the intersatellite range from the phase measurements for each epoch. The flowcharts for the two procedures are shown Figs. 2 and 3.

1) The first step generates truth orbits with truth dynamic models, that is, gravity and drag models. These orbits provide the two satellites' positions as a function of nominal time, and this truth instantaneous range at each nominal time is saved for later comparison. Furthermore, GPS observations of two satellites are generated along the truth orbits.

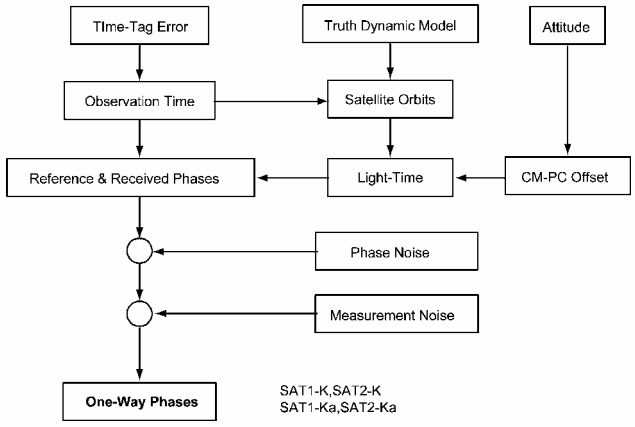

Fig. 2 Generation procedure of one-way phase measurements.

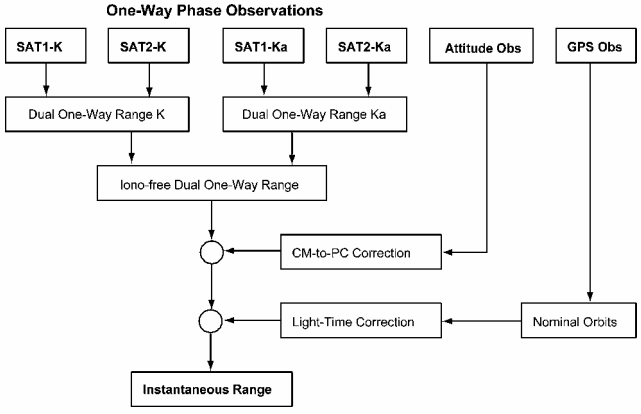

Fig. 3 Processing procedure of dual one-way phase measurements.

2) The time-tag errors are generated and added to the nominal time to yield the actual observation (signal reception) time. By a conventional iteration method, the TOF of the carrier signal corresponding to the observation time can be approximated from the satellite positions. This TOF includes the geometric range, ionosphere phase advance, and antenna offset. The transmit time is computed by subtraction of the TOF from the observation time.

3) The phase error time series are generated from the oscillator specification. The transmit phase, which is the sum of nominal phase and phase error, is computed at each transmit time, and this phase becomes the received phase at the observation time. The receiver reference phase is generated at the observation time. The phase measurements were computed by subtraction of the received phase from the reference phase and by addition of the measurement noise described earlier. Four one-way phase measurements of Eq. (2) are computed for the two satellites and two frequency bands.

4) To process the dual one-way measurements, a set of nominal orbits is required for the light-time and other corrections. With nominal dynamic models, these orbits can be estimated from the GPS observations generated in step 1.

5) For each frequency band, the two carrier phase measurements are combined to form a dual one-way phase measurement by the use of Eq. (3), and these phase quantities are converted to the dual one-way range measurements.

6) The K and K_a range measurements are combined to obtain the ionosphere-free dual one-way range by the use of Eq. (9). The light-time and c.m.-to-PC corrections convert the dual one-way measurement into the instantaneous range, where the light-time correction is computed from the nominal orbits. The measurement bias, for example, phase ambiguity, still remains during this process.

7) The computed instantaneous range is compared with the truth instantaneous range of step 1 (except the measurement bias). This difference represents the expected intersatellite range error. Because the bias can be fully removed by adjustment of appropriate empirical parameters during the orbit and gravity estimation process, the bias level is not included in the error analysis.

Simulation Description

The GRACE satellite models were used for the simulations, and the following sections describe the dynamic and measurement models.

Data Description

A typical mission orbit was selected for the simulation, and one-day's worth of data were simulated with 10-s intervals. Table 1 describes the simulation data type and error models. One satellite's frequencies were higher than the other satellite's by 0.5 MHz in both the K and K_a bands.

Dynamic Models

Two sets of dynamic models, truth and nominal, were used for the measurement generation and processing, respectively. The difference between these two models represents the current uncertainty level of the dynamic models.

Truth dynamic models, used for generation of the truth orbit trajectories, consist of the gravitational and nongravitational models. The EGM96 Earth gravity model,[12] which is a set of spherical harmonic coefficients, was used as the truth gravitational model. To realize the high-frequency feature of the gravity accelerations, degree and order 360 gravity coefficients were applied. Atmospheric drag and radiation pressure were applied to model the nongravitational accelerations.

For the nominal orbit estimation, the simulated GPS measurements were processed with nominal dynamic models.[13] The difference (1σ) between the truth and nominal orbits were 50 cm in position and 5 cm/s in velocity. These differences are conservative when compared with current GPS orbit determination accuracy.

Measurement Error Models

The GRACE satellites use a quartz crystal type ultrastable oscillator. From its Allan deviations, a set of state-space equations was derived and used for integration of the phase error time series.[14,15] The two oscillators had the same noise power spectrum, but different error realizations, by the use of different seed numbers for the random number generation.

Table 1 Simulation description

Type	Parameters
Data description	
Measurement type	Four one-way carrier phases for each epoch
Phase frequency bands	K (24 GHz), K_a (32 GHz)
Frequency offset	For K and K_a, 0.5 MHz
Estimation parameter	One instantaneous range for each epoch
Sampling interval	10 s
Data span	1 day
Orbit conditions	
Altitude	450 km
Separation distance	239 km
Eccentricity	0.001
Inclination	87 deg
Dynamic error	
Dynamic models	Gravity, atmospheric drag, solar, and Earth radiation pressure
Position error (1σ)	50 cm
Velocity error (1σ)	5 cm/s
Measurement error	
Oscillator noise	Allan variance 2×10^{-13} for 100 s
Time-tag error	200-ps relative variation (1σ)
System noise	$C/N_0 = 69$ dB · Hz at 220 km
Multipath error	3-μm/mrad attitude variation
AM/PM error	0.01 cycles per revolution
Attitude control error	0.5 mrad (yaw, pitch)
Attitude knowledge error	0.05 mrad
Thermal variation	Sum of harmonics or input time series (not included in the simulations)

The absolute time-tag error for each satellite was modeled to have a standard deviation of 141 ps. Because the two satellites' time-tag errors were modeled to be independent, the relative time-tag error was 200 ps ($200 = \sqrt{2} \times 141$). With the GPS and International GPS Service network data, this accuracy level can be achieved without significant difficulties. This is especially true of the relative time-tag error because most of the common error sources cancel.

The system noise $\varepsilon_{\text{system}}$ was approximated as white noise for the one-way phase measurement. Its standard deviation corresponds to the C/N_0 (signal/noise spectral density) value of 69 dB · Hz, predicted for the nominal separation distance (~220 km) (Ref. 8).

It is hard to develop a general model of the multipath effects because of the arbitrarily different geometric situations. However, with some approximations made by Thomas[8] (see also Ref. 11), it is possible to derive a simple relationship between the attitude variation and a pessimistic multipath error model. With these approximations, the multipath error $\varepsilon_{\text{multipath}}$ was modeled as proportional to the attitude error variation and signal reduction factor. The attitude simulation results from NASA Langley Research Center/Analytic Mechanics Association, Inc.,[16,17] were used to realize the attitude control error, that is, microwave boresight deviation from the true LOS. The reduction factor around the front edge was assumed to be −50 dB. With these conditions, a 1-mrad attitude control error yields an approximately 3-μm range error.

The AM/PM conversion error was modeled proportional to the signal travel length, or the intersatellite distance. As with the range variation, the most dominant AM/PM error signal is the one cycle per revolution component with an amplitude of 0.01 cycle. The high-frequency variation of this error is much smaller than the low-frequency variations.

The c.m.-to-PC offset computation requires two attitude time series: truth and nominal. The same attitude time series used to produce the multipath error was used for the truth case. This angle was combined with the truth c.m.-to-PC distance to provide the c.m.-to-PC offset d_{true}. The nominal attitude time series was obtained by addition of the attitude knowledge error (modeled as white noise) to

the truth attitude time series. The nominal c.m.-to-PC offset d_{nominal} was obtained from the nominal attitude and c.m.-to-PC distance.

Simulation Results

This section describes the output from each simulation step and presents an analysis of the results. In addition to the standard simulation, which utilized the simulation parameter in Table 1, another set of sensitivity studies were performed by changing some parameters.

Figure 4 shows the intersatellite range time series computed from the truth orbits. Because the timescale is short, the secular effect that dominates the long-term signal has been removed. Accurate estimation of this range from the phase measurements is the objective for this part of the processing. One orbit period is approximately 5600 s, and so the one cycle per revolution frequency becomes 1.8×10^{-4} Hz. The range time series shows a strong one cycle per revolution signal with the amplitude of 1 km, and this is mainly a consequence of the nonzero orbit eccentricity.

The phase noise time series of the two oscillators are shown Fig. 5. Each time series was generated for the base frequency (5 MHz) and then scaled to the carrier frequency (K band) phase errors. Because the same oscillators are used for both K and K_a band carrier frequencies, the phase errors for the K_a band have the same variability, but different amplitude. These errors were applied to the truth reference and received phases.

Figure 6 shows the time series of the four one-way phase measurements for the two satellites and two frequency bands. These one-way phases are the output of the measurement generation in simulation step 3. Because of the frequency offset between the two satellites, one set of measurements increases linearly, whereas the other decreases linearly. In the case of the actual mission, a phase-locked loop will be reset periodically to avoid the overflow of the phase measurements after a certain period. In this simulation, high-precision numbers (16-B real) were used to minimize the loss of accuracy. No phase ambiguities were applied to these measurements.

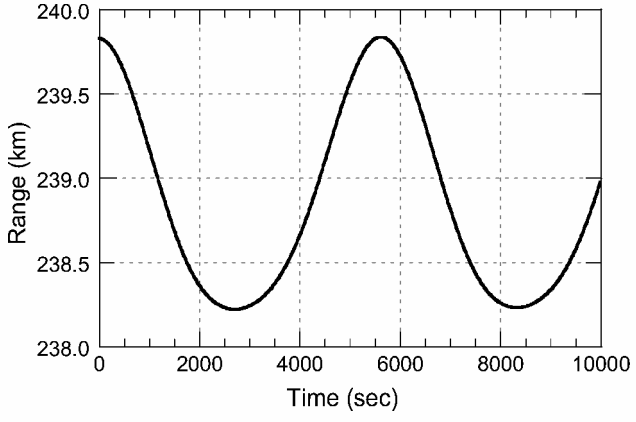

Fig. 4 Truth intersatellite range time series.

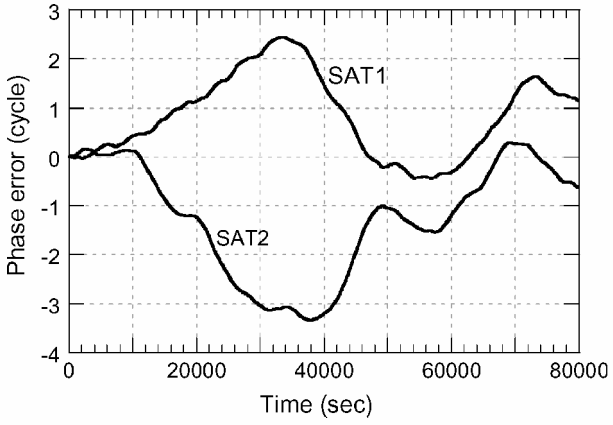

Fig. 5 Phase error time series of two oscillators.

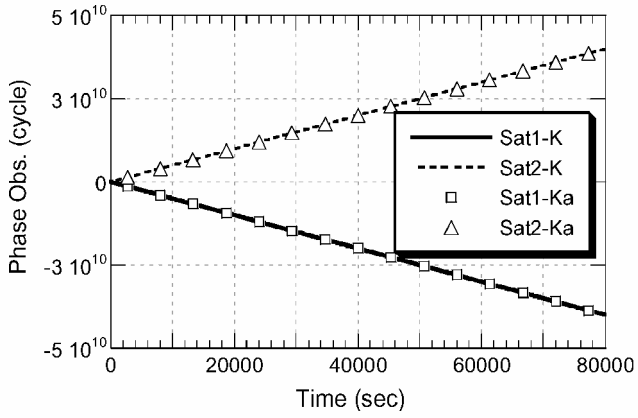

Fig. 6 One-way phase measurements.

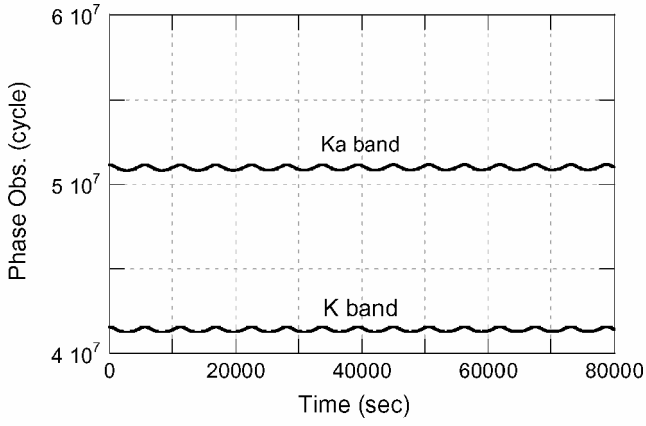

Fig. 7 Dual one-way phase measurements.

Because the phase ambiguity can be fully absorbed by use of empirical parameters during the estimation process, the presence of the ambiguity has a negligible effect on the measurement accuracy.

Figure 7 shows the dual one-way phases for the K and K_a bands. They are the sum of the two one-way measurements in Fig. 6. The K and K_a phases have different cycles because of their wavelength and ionosphere delay differences. Both measurements show strong one-cycle-per-revolution signals, as with the range variation. These dual one-way phase measurements were converted into the dual one-way range by multiplication of their wavelengths from Eq. (7). The ionosphere-free range was obtained by combination of those two frequency band ranges and their conversion into the instantaneous range by application of the light-time corrections computed from the nominal orbits. Another simulation result proved that the nominal orbit accuracy is not sensitive to the light-time correction accuracy and that the effect of the light-time correction error is negligible in comparison to other error sources.

The range error time series is illustrated in Fig. 8. This is the difference between the truth and estimated instantaneous ranges. The error level is very low, rms of 1.7 μm, when the large oscillator instability is considered. The dominant variation is the one cycle per revolution variation because some of the error sources are proportional to the range variation that has a strong one cycle per revolution variation.

The power spectrum of the range error is shown in Fig. 9. At the high frequency, the error level is close to 1 $\mu\text{m}/\sqrt{\text{Hz}}$, which is the system noise level. Its low-frequency noise level is higher and is mainly due to the strong low-frequency signal of the oscillator noise residual. For comparison, the range error spectrum without the dual-one way ranging is also included in Fig. 9. This single one-way ranging error was obtained by multiplication of the one-way phase measurement error by its wavelength. This ranging error level is comparable to the conventional phase-derived ranging error level before the oscillator error adjustment is applied. This

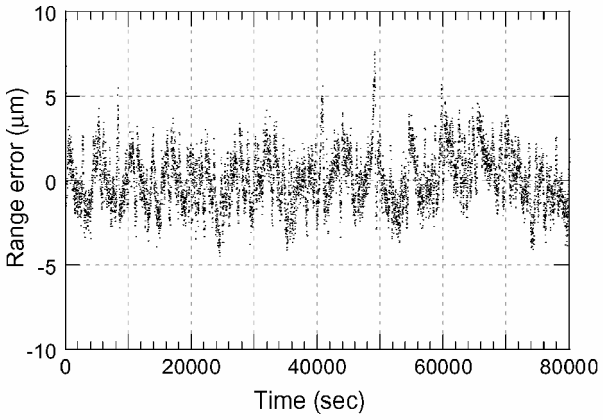

Fig. 8 Instantaneous range error (truth-estimated).

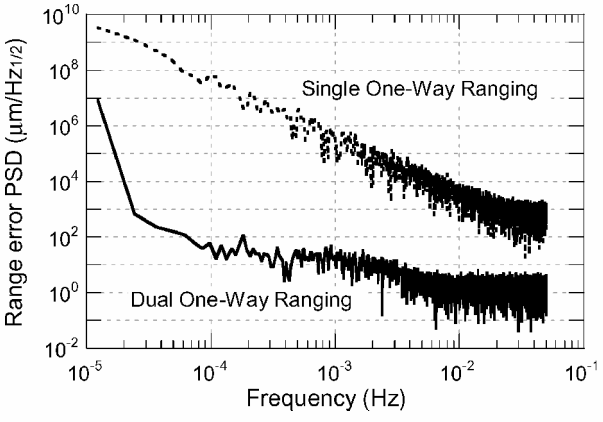

Fig. 9 Comparison of the range error power spectra, dual one-way vs single one-way ranging.

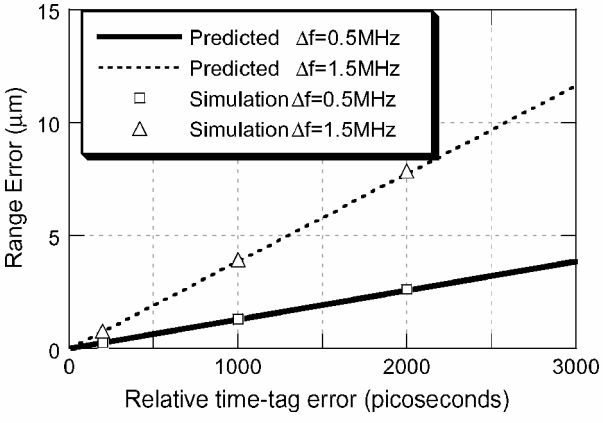

Fig. 10 Effect of the relative time-tag error on the ranging accuracy.

comparison shows how much reduction can be achieved with the dual one-way ranging system where noise reduction on the order of 10^6 was obtained for low frequency. This reduction, or the noise level difference, is less significant for high-frequency noise because the dual one-way ranging system is more effective at removing the low-frequency oscillator noise.

Figure 10 illustrates the effect of the relative time-tag error on the ranging accuracy by changes made in the time-tag error level. The predicted error level was computed from the third term of Eq. (5), and the simulated results agree with the predicted level very well. Because the error effect depends on the frequency offset between the two satellites as well, the 1.5-MHz offset was tested in addition to the 0.5-MHz offset. The result proves that the smaller frequency offset provided a better ranging accuracy.

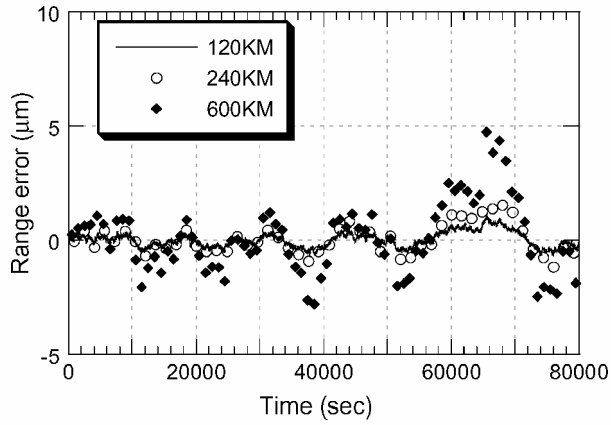

Fig. 11 Effect of the separation distance on the ranging accuracy.

Figure 11 shows the range error level variation along the separation distance changes. Three distances, 120, 240, and 600 km, were tested, and no measurement errors except the oscillator noise were applied. The range error level is almost linearly proportional to the separation distance or the signal TOF because the dual one-way ranging filtering performance (reduction of the oscillator noise) decreased as the TOF increased. This relationship suggests that a short separation distance is better for reduction of the oscillator noise. A shorter distance reduced the other instrument noise levels as well, for example, system, AM/PM, etc. When the range error level variation was analyzed in the spectral domain (not shown in this paper), it showed nearly the same amount of increase over all of the frequency range as the separation distance increased.

The simulation results matched the GRACE hardware test results, performed by the JPL GRACE team, but two results were not directly comparable because of different testing conditions, for example, time synchronization accuracy, thermal variation, etc. More comprehensive and actual hardware performance analysis will be available when the flight data are analyzed. A preliminary analysis on the initial flight data of the GRACE GPS receivers and dual one-way ranging system are described in Ref. 18.

The range-rate signal can be obtained by passage of the range signal through a differentiation filter. The accuracy of the range-rate signal depends heavily on the filtering scheme. The GRACE data processing team has been testing various differentiation filters, and the details are described in Ref. 8. Overall accuracy of the range rate is well below 1 μm/s, which is comparable to the GRM engineering model test results.[1] However, direct comparison between the GRACE and GRM dual one-way ranging system performance is not possible because the two systems have different oscillators, carrier frequencies, and measurement types, etc.

Conclusions

A high-accuracy intersatellite ranging system for the GRACE mission was described. The measurement equations have been derived to show how the dual one-way ranging system removes most of the oscillator noise component effectively. Most of the significant error sources were discussed, and their implementation of the software simulator was described. The simulation results demonstrate that a very high accuracy of intersatellite range measurement can be achieved by the use of the dual one-way ranging system. This simulation tool was useful in identification of the effect of individual error sources and was used to test the GRACE ground data processing algorithm. This tool can be used for other dual one-way ranging systems when the simulation parameters are changed.

Acknowledgments

The authors thank Kevin W. Key at the University of Texas (now at LinCom Corp.) and J. Brooks Thomas at Jet Propulsion Laboratory, California Institute of Technology (now retired), for providing a basis of this research. The authors are pleased to acknowledge

the significant contributions of the Gravity Recovery and Climate Experiment team members around the world.

References

[1]MacArthur, J. L., and Posner, A. S., "Satellite-to-Satellite Range-Rate Measurement," *IEEE Transactions on Geoscience and Remote Sensing*, Vol. GE-23, No. 4, 1985, pp. 517–523.

[2]Pisacane, V. L., Ray, J. C., MacArthur, J. L., and Bergeson-Willis, S. E., "Description of the Dedicated Gravitational Satellite Mission (GRAVSAT)," *IEEE Transactions on Geoscience and Remote Sensing*, Vol. GE-20, No. 3, 1982, pp. 315–321.

[3]Yionoulis, S. M., and Pisacane, V. L., "Geopotential Research Mission: Status Report," *IEEE Transactions on Geoscience and Remote Sensing*, Vol. GE-23, No. 4, 1985, pp. 511–516.

[4]Wolff, M., "Direct Measurements of the Earth's Gravitational Potential Using a Satellite Pair," *Journal of Geophysical Research*, Vol. 74, No. 22, 1969, pp. 5295–5300.

[5]Keating, T. P., Taylor, P., Kahn, W., and Lerch, F., "Geopotential Research Mission, Science, Engineering, and Program Summary," NASA TM-86240, 1986, pp. 69–73.

[6]Reigber, Ch., Schwintzer, P., Hartl, Ph., IIk, K. H., Rummel, R., van-Geldern, M., Schrama, E. J. O., Wakker, K. F., Ambrosius, B. A. C., and Leenman, H., "Study of a Satellite-to-Satellite Tracking Gravity Mission," European Space Research and Technology Centre, ESA CR 6557/85/NL/pp(SC), Munich, March 1987, pp. 15–43.

[7]Davis, E. S., Dunn, C. E., Stanton, R. H., and Thomas, J. B., "The GRACE Mission: Meeting the Technical Challenges," International Astronautical Federation, Paper IAF-99-B.2.05, Oct. 1999.

[8]Thomas, J. B., "An Analysis of Gravity-Field Estimation Based on Intersatellite Dual-1-Way Biased Ranging," Jet Propulsion Lab., California Inst. of Technology, JPL Publication 98-15, Pasadena, CA, May 1999.

[9]Sharma, J., "Precise Determination of the Geopotential with a Low–Low Satellite-to-Satellite Tracking Mission," Ph.D. Dissertation, Dept. of Aerospace Engineering and Engineering Mechanics, Univ. of Texas, Austin, TX, Dec. 1995.

[10]Leick, A., *GPS Satellite Surveying*, 2nd ed., Wiley, New York, 1995, pp. 247–271.

[11]Kim, J., "Simulation Study of a Low–Low Satellite-to-Satellite Tracking Mission," Ph.D. Dissertation, Dept. of Aerospace Engineering and Engineering Mechanics, Univ. of Texas, TX, May 2000.

[12]Lemoine, F. G., Kenyon, S. C., Factor, J. K., Trimmer, R. G., Pavlis, N. K., Chinn, D. S., Cox, C. M., Klosko, S. M., Luthcke, S. B., Torrence, M. H., Wang, Y. M., Williamson, R. G., Rapp, R. H., and Olson, T. R., "The Development of the Joint NASA/GSFC and the National Imagery and Mapping Agency (NIMA) Geopotential Models, EGM96," NASA TP-1998-206861, July 1998, pp. 1–3.

[13]Kim, J., and Tapley, B. D., "Error Analysis of a Low–Low Satellite-to-Satellite Tracking Mission," *Journal of Guidance, Control, and Dynamics*, Vol. 25, No. 6, 2002, pp. 1100–1106.

[14]Meditch, J. S., "Clock Error Models for Simulation and Estimation," The Aerospace Corp., Aerospace Rept. TOR-0076 (6474-D1)-2, El Segundo, CA, July 1975.

[15]Kosaka, M., "Evaluation Method of Polynomial Models' Prediction Performance for Random Clock Error," *Journal of Guidance, Control, and Dynamics*, Vol. 10, No. 6, 1987, pp. 523–527.

[16]Stevens, H. D., Rodden, J., and Carrou, S., "Mass Expulsion Control for Precision Pointing Spacecraft," *Advances in the Astronautical Sciences*, Vol. 103, 2000, pp. 297–304.

[17]Mazanek, D. D., Kumar, R. R., Seywald, H., and Min, Q., "GRACE Mission Design: Impact of Uncertainties in Disturbance Environment and Satellite Force Models," *Advances in the Astronautical Sciences*, Vol. 105, 2000, pp. 967–986.

[18]Dunn, C., Bertiger, W., Bar-Sever, Y., Desai, S., Haines, B., Kuang, D., Franklin, G., Harris, I., Kruizinga, G., Meehan, T., Nandi, S., Nguyen, D., Rogstad, T., Thomas, B., Tien, T. J., Romans, L., Watkins, M., Wu, S.-C., Bettadpur, S., and Kim, J., "Application Challenge: Instrument of Grace GPS Augments Gravity," *GPS World*, Vol. 14, No. 2, 2003, pp. 16–28.

D. L. Edwards
Associate Editor